Title:	Limit Analysis for Punching Shear Design of Compact Slabs and Footings
Authors:	Simões J. T., Faria D. M. V., Muttoni A., Fernández Ruiz M.
Published in:	fib Symposium
Pages:	13 p.
City, country:	Copenhagen, Denmark
Year of publication:	2015
Type of publication:	Peer reviewed conference paper

Please quote as:	Simões J. T., Faria D. M. V., Muttoni A., Fernández Ruiz M., *Limit Analysis for Punching Shear Design of Compact Slabs and Footings*, fib Symposium, Copenhagen, Denmark, 2015, 13 p..

LIMIT ANALYSIS FOR PUNCHING SHEAR DESIGN OF COMPACT SLABS AND FOOTINGS

João T. Simões, Duarte M. Viúla Faria, Aurelio Muttoni and Miguel Fernández Ruiz

Ecole Polytechnique Fédérale de Lausanne, ENAC, CH-1015 Lausanne, Switzerland

Abstract

In this paper, the kinematical theorem of limit analysis is used to obtain the governing failure mechanisms and the corresponding failure load of reinforced concrete footings without transverse reinforcement. To that purpose, a Mohr-Coulomb yield criterion is used for the concrete together with uniaxial rigid-plastic behaviour for the reinforcing bars. Two different mechanisms allowing failures with both rotational and translational movements are used. The results show that various failure modes can develop, associated to clockwise or counter-clockwise rotations combined with translational movements. It is also shown that a flexural-shear regime, representing a transition between pure flexural and punching shear failures may be governing, with a lower load carrying capacity than a pure flexural failure mechanism. Finally, it is shown that the failure mechanism governing in the punching shear regime might be dependent on the amount of top compression reinforcement. A fairly good agreement is found between theoretical and experimental results.

Keywords: Compact slabs, footings, flexural-shear, punching shear, limit analysis, plastic theory

1 Introduction

Limit analysis is a consistent tool for design of reinforced concrete members provided that the behaviour is sufficiently ductile. This is for instance the case of beams with transverse reinforcement, where the influence of smeared cracking on the concrete strength is usually considered in a simplified manner by means of an efficiency (or strength reduction) factor. In case crack localization develops, the deformation capacity of the member is reduced. In these cases, the use of limit analysis is still possible, yet the influence of crack development on the compressive strength of concrete is to be carefully accounted and other phenomena govern (such as size effect). This is corresponds for example to the case of punching shear failures near concentrated loads. Regardless of the presence of transverse reinforcement, strains localize near the concentrated loads due to the relatively strong gradients of bending moments and shear forces and a single critical shear crack develops. Investigations of the punching shear strength have shown that for relatively high levels of shear force (as for compact footings or for flat slabs with large amounts of transverse reinforcement), crushing of the concrete struts is governing for the punching strength. For these cases, application of limit analysis is possible provided that the influence of cracking is suitably considered on the concrete strength.

The load carrying capacity of footings has been investigated by several researchers (e.g. Talbot 1913; Richart 1948; Kordina & Nölting 1981; Dieterle 1986; Dieterle & Rostásy 1987; Hallgren, Kinnunen & Nylander 1998; Hallgren & Bjerke 2002; Timm 2003; Hegger, Sherif & Ricker 2006; Hegger & al. 2007; Hegger, Ricker & Sherif 2009; Ricker 2006; Siburg & Hegger 2014; Urban & al. 2013). Nevertheless, there is yet no consensus about a mechanical model to determine the load carrying capacity of these elements when subjected to concentrated loads. In this paper, limit analysis is used to obtain the governing failure mechanisms and load carrying capacity of reinforced concrete footings without transverse reinforcement.

Limit analysis was firstly applied to reinforced concrete elements subjected to in-plane shear by Drucker (1961), who proposed a stress field (Fig. 1(a)) and a failure mechanism (Fig. 1(b)) providing

the same strength, therefore corresponding to the exact plastic solution. Thereafter, limit analysis has been used to investigate the shear strength of several plain and reinforced concrete elements (e.g. Johansen 1962; Gesund & Dikshit 1971; Braestrup 1974, 1979, 1981; Jensen 1975; Braestrup & al. 1976; Nielsen & al. 1978; Nielsen, Braestrup & Jensen 1978; Gesund 1983, 1985; Jiang and Shen 1986; Bortolotti 1990; Kuang 1991; Salim & Sebastian 2002; Chen 2007; Nielsen & Hoang 2011). With respect to the punching shear strength of slabs, Braestrup & al. (1976) proposed a kinematical approach based on a failure mechanism consisting on a vertical shift of the outer portion of the slab (refer to Fig. 1(c)), considering a modified Coulomb failure criterion for the concrete. Jiang & Shen (1986), Bortolloti (1990), Kuang (1991) and Sebastian & Salim (2002) have also presented others solutions based on the kinematical theorem of limit analysis, considering the same failure mechanism originally proposed by Braestrup & al. (1976), but with some differences, notably, in the concrete behaviour. Using the referred failure mechanism (Fig. 1(c)), the mentioned works have neglected the influence of rotations at failure (and thus the influence of both bottom and top reinforcement), therefore allowing only the analysis of punching shear regime.

A rational approach based on the kinematical theorem of limit analysis is presented in this paper, referring specifically to the cases of compact slabs and footings with concentrated reactions. The approach presented is nevertheless also applicable to the case of footings with different distributions of reactions (as for example uniform soil reaction). Two potential failure mechanisms are considered. Both mechanisms result from a relative rotation rate around an instantaneous centre of rotation. The kinematics considered differ in the admissible location for the instantaneous centre of rotation as well as in the direction of the rotation considered. The solution presented in this paper considers therefore the influence of rotations activating both the bottom and the top reinforcement, allowing the analysis not only of punching shear failures, but also of flexural and combined flexural-shear failures. The results are finally discussed and compared to some available experimental evidence.

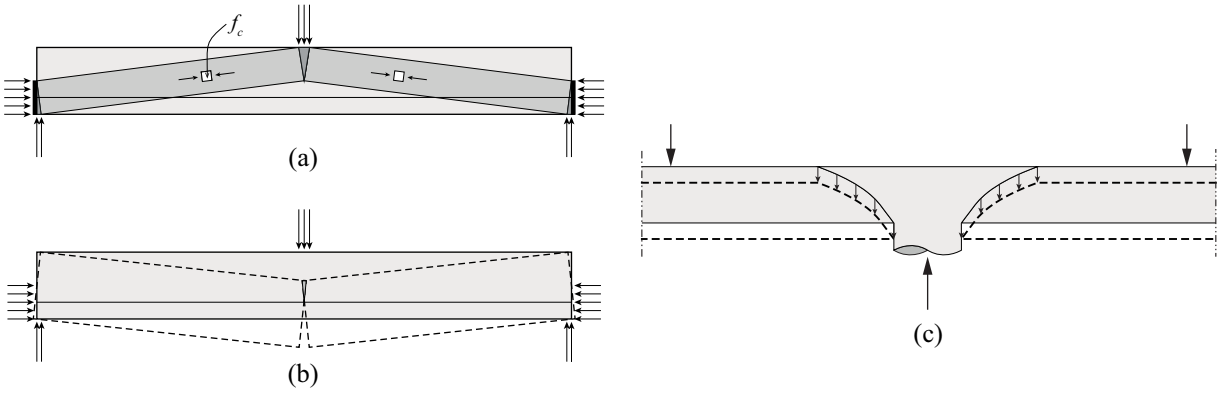

Fig. 1 First application of limit analysis to reinforced concrete elements subjected to in-plane shear by Drucker (1961) through the development of a (a) stress field and (b) a kinematically admissible mechanism; (c) kinematically admissible mechanism originally proposed by Braestrup & al. (1976) to calculate the punching shear strength of slabs.

2 Kinematical theorem of limit analysis applied to footings

The kinematical theorem of limit analysis will be used in this work. This theorem states that the rate of internal energy dissipated has to be balanced by the rate of external work. The materials are considered to behave in a perfectly rigid-plastic manner. As shown in Fig. 2(a), uniaxial rigid-plastic behaviour in both tension and compression is considered for the reinforcement. A Mohr-Coulomb yield criterion is used for the concrete, being the tensile strength neglected (tension cut-off of plasticity surface) due to its brittle behaviour (refer to Fig. 2(b) and (c)). A plastic compressive strength of concrete is also considered (Muttoni 1990; Muttoni, Schwartz & Thürlimann 1997; Fernández & Muttoni 2007, 2008):

$$f_{cp} = f_c \cdot \eta_\varepsilon \cdot \eta_{fc} \tag{1}$$

where the reductions factors η_ε and η_{fc} take into account, respectively, the potential presence of transverse strains and the brittle behaviour in compression of high-strength concrete. The latter factor may be computed as (Muttoni 1990; Muttoni, Schwartz & Thürlimann 1997; Fernández & Muttoni 2007, 2008):

$$\eta_{cp} = \left(\frac{f_{c0}}{f_c} \right)^{1/3} \leq 1 \tag{2}$$

With respect to the reduction factor accounting for the presence of transverse strains η_ε, it is important to note that it may be evaluated according to several formulations (e.g. Vecchio & Collins 1986, 1988; Collins & al. 1996; Muttoni 1990; Muttoni, Schwartz & Thürlimann 1997; Vecchio 2000). Other researchers consider both reductions factors together $\eta=\eta_\varepsilon\eta_{fc}$, proposing a global efficiency factor (e.g. Nielsen & Hoang 2011).

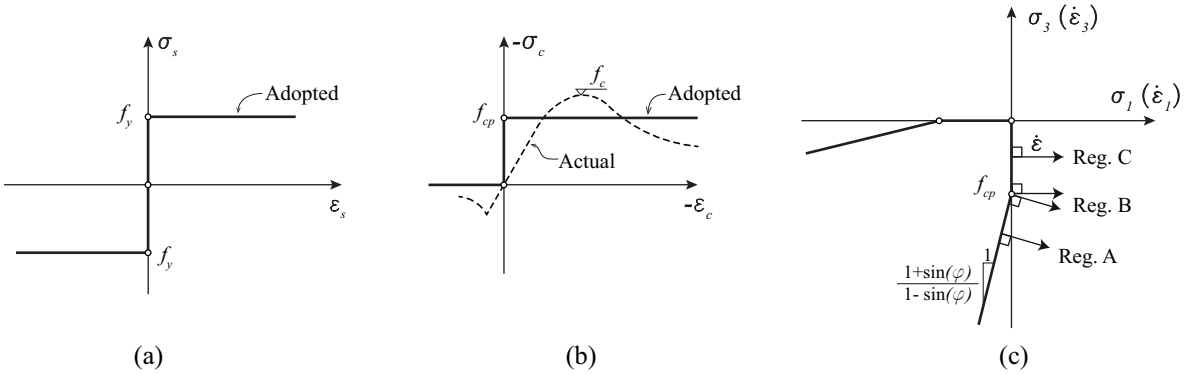

(a) (b) (c)

Fig. 2 (a) Rigid-plastic behaviour both in tension and compression admitted for the reinforcement bars; (b) rigid-plastic behaviour considered for concrete; (c) Mohr-Coulomb failure criterion adopted for concrete.

The geometry of a compact footing is presented in Fig. 3(a): (i) r_s represents the radius of the footing; (ii) r_c is the radius of the column; (iii) r_q is the radius of the introduction of the reaction resultant; (iv) r_0 is the radius of the failure surface at the level of bottom flexural reinforcement; (v) d is the effective depth of the bottom reinforcement, which is assumed to be the distance between the centroid of the bottom reinforcement and the top surface of the footing; (vi) d' is the effective depth of the top reinforcement; (vii) h is height of the footing; (vii) ρ and ρ' are respectively the bottom and top reinforcement ratios. With respect to materials properties (besides the plastic concrete compressive strength f_{cp}) f_y and f_y' are respectively considered as the yield strength of the bottom flexural and top reinforcement.

A narrow plastic zone, developing along the entire effective depth of the footing separates it in two portions. The velocity $\dot{u}$ in each infinitesimal part of this narrow plastic zone results from the relative rotation rate $\dot{\psi}$ around an instantaneous centre of rotation, see Fig. 4(b) and (c):

$$\dot{u} = \sqrt{\left(r - r_{ICR}\right)^2 + \left(z - z_{ICR}\right)^2} \cdot \dot{\psi} \tag{3}$$

The radial component of this velocity may be computed as:

$$\dot{u}_r = \left| z - z_{ICR} \right| \cdot \dot{\psi} \tag{4}$$

While the inner portion is considered rigid, the outer portion is considered to deform according to a conical shape due to compatibility reasons of the velocity field occurring along the failure surface (which is considered to be rotationally symmetric). As a result, dissipation of energy due to tangential bending may occur and is taken into account. As shown in Fig. 6(b) and (c), two different mechanisms (corresponding to two different kinematics) named M1 and M2 are considered. The admissible

location for the instantaneous centre of rotation, as well as the direction considered for the rotation, distinguishes both mechanisms. The mechanism leading to the lowest load carrying capacity is the governing one, representing the upper bound of the load carrying capacity.

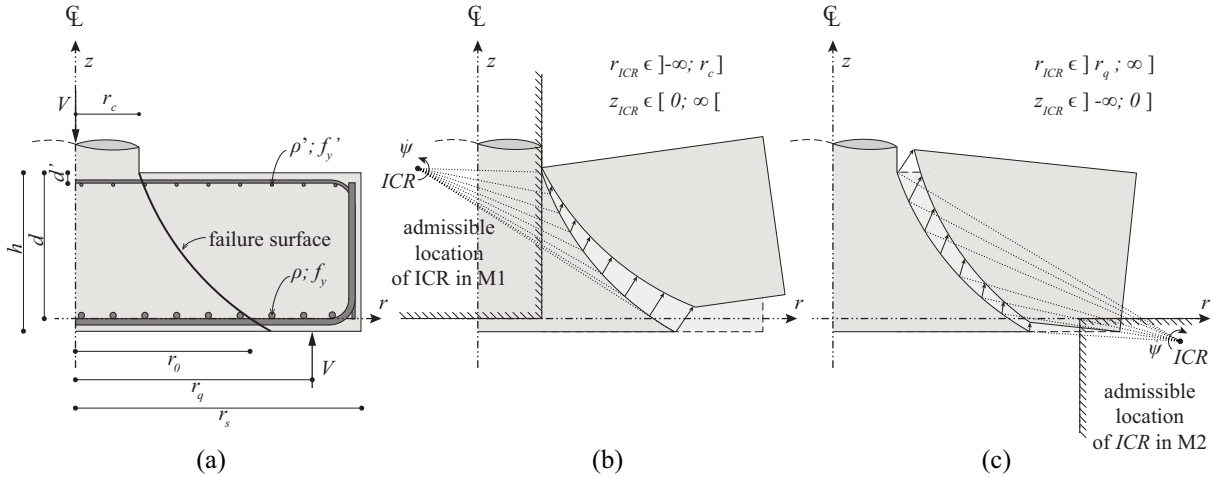

Fig. 3 (a) Definition of geometrical parameters and materials properties used in the proposed approach; admissible location of the instantaneous centre of rotation for mechanism (b) M1 and (c) M2.

As shown in Fig. 3(b), mechanism M1 represents a kinematics characterized by a counter-clockwise rotation with an instantaneous centre of rotation radially located behind the edge of the column and vertically located above the bottom flexural reinforcement. When the instantaneous centre of rotation is close to the tip of the failure surface and below the top surface, a significant rotation is observed in the failure mechanism with the development of a tangential compression zone (resulting from the conical deformed shape of the outer zone), indicating flexural failures. On the other hand, if the instantaneous centre of rotation shifts to infinite ($r_{ICR} \rightarrow -\infty$), a vertical translational movement characterizes the failure mechanism. This is the failure mechanism originally proposed by Braestrup & al. (1976) for punching failures of flat slabs. In this latter case, the load carrying capacity is only dependent on the rate of internal energy dissipated along the failure surface.

The kinematics considered in mechanism M2 presents a clockwise rotation with an instantaneous centre of rotation radially located beyond r_q (the radius where the reaction is applied) and vertically located below the bottom flexural reinforcement (refer to Fig. 3(c)). This kinematics is associated with punching shear failures, since it not only enables the development of a failure mechanism without activation of bottom reinforcement, but also considers a rotation direction opposite to the one known to occur in flexural failures. When the instantaneous centre of rotation is radially located at infinite, the failure mechanism given by this kinematics is again characterized by a vertical shift of the outer portion of the footing, corresponding again to the failure mechanism presented by Braestrup & al. (1976).

An example of failure mechanisms (a) M1 and (b) M2 with their corresponding velocity fields is shown in Fig. 4. The definition of the location of the instantaneous centre of rotation (r_{ICR}, z_{ICR}) and the geometry of the failure surface, defined by the function *r(z)*, enables the computation of each component of the total rate of internal energy dissipation and rate of external work, therefore allowing the calculation of the load carrying capacity. The rate of external work is only given by the reaction resultant, while the total rate of internal energy dissipation results from the sum of different components, namely, energy dissipated along the failure surface, energy dissipated in concrete due to tangential bending of the outer footing portion and, finally, the energy dissipated in both bottom and top reinforcements. Each component may be calculated as explained in the following.

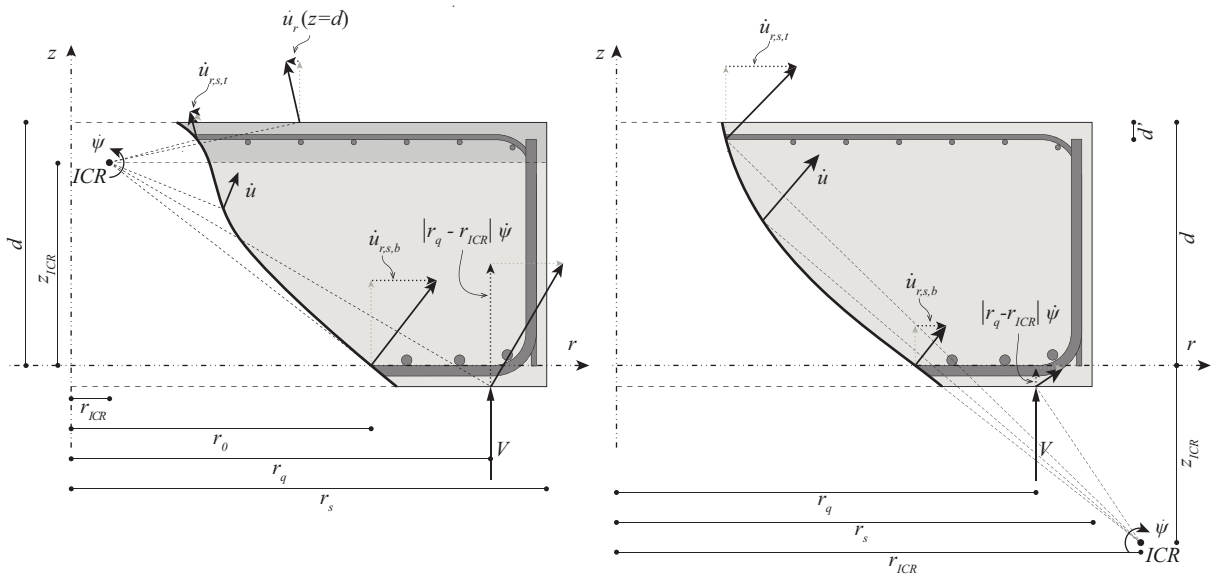

Fig. 4 Example of mechanism (a) M1 and (b) M2 with corresponding velocity fields.

3.1 Rate of external work

The rate of external work P_e, whose only source is the reaction resultant, is given by:

$$P_e = V \cdot \left| r_q - r_{ICR} \right| \cdot \dot{\psi} \tag{5}$$

The rate of external work is always a non-negative scalar. In the case of concentrated reactions, as the case in study, V represents the concentrated reaction located at a radius r_q from the centre of the footing. In the case of concentrated reactions, the failure surface may reach the level of bottom flexural reinforcement in between the column edge and the reaction inner radius.

3.2 Rate of internal energy dissipated in the concrete along the failure surface

A radial view of an infinitesimal part of the narrow plastic zone with a thickness Δ developing along the failure surface is shown in Fig. 5(b). It is still considered that the failure surface develops only between the level of bottom flexural reinforcement and top surface, being the concrete cover contribution of the bottom reinforcement neglected. Based on the mentioned assumptions, the rate of internal energy dissipated along the failure surface may be calculated as:

$$P_{i,c,FS} = -\pi \cdot f_{cp} \cdot \int_0^d \left[\sin(\chi) - 1\right] \cdot \dot{u} \cdot r \cdot \frac{dz}{\sin(\alpha)} \tag{6}$$

where α represents the angle between the failure surface and the vertical axis; χ refer to the angle between the failure surface and the velocity $\dot{u}$. The calculation of this component was already shown by several researchers (e.g. Jensen 1975) and applied previously to punching shear problems assuming $\chi = \alpha$ (Braestrup 1979; Braestrup & al. 1976). Substituting (3) in (6), the rate of internal energy dissipated along the failure surface may be obtained by:

$$P_{i,c,FS} = -\pi \cdot f_{cp} \cdot \dot{\psi} \cdot \int_0^d \left[\sin(\chi) - 1\right] \cdot \sqrt{\left(r - r_{ICR}\right)^2 + \left(z - z_{ICR}\right)^2} \cdot r \cdot \frac{dz}{\sin(\alpha)} \tag{7}$$

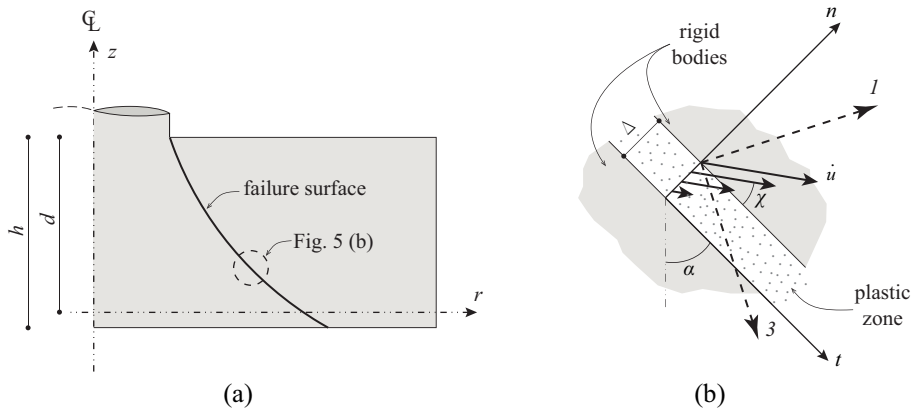

(a) (b)

Fig. 5 (a) Representation of failure surface and (b) radial view of infinitesimal part of narrow plastic zone occurring along the failure surface.

The consideration of the Mohr-Coulomb yield criterion with a tension cut-off leads to the definition of three potential regimes occurring along the failure surface (refer to Fig. 2 (b)): (i) Regime A ($\chi = \varphi$) , where the rate of internal energy dissipated per unit area is maximum, therefore corresponding to a sliding failure; (ii) Regime B ($\varphi < \chi < 90°$), where the rate of internal energy dissipated per unit of area is non-zero; (iii) Regime C ($\chi = 90°$), where no dissipation of energy occurs (since tensile strength is neglected), representing a separation failure.

3.3 Rate of internal energy dissipated in the concrete tangential compression

As previously explained, when the instantaneous centre of rotation is below the top surface in mechanism M1 ($0 < z_{ICR} < d$), a tangential compression zone develops in the outer portion of the footing in between $z_{ICR} < z \leq d$ (refer to Fig. 4(a)). In this case, the rate of internal energy dissipated due to tangential compression is given by:

$$P_{i,c,t} = -\int \dot{\varepsilon}_{c,t} \cdot f_{cp} \cdot dVol \tag{8}$$

where the unit of volume $dVol$ and the corresponding strain rate $\dot{\varepsilon}_{c,t}$ (given by the ratio of the radial component of the velocity and the radius) are respectively given by:

$$dVol = dA \cdot dz = r \cdot dr \cdot d\vartheta \cdot dz \tag{9}$$

$$\dot{\varepsilon}_{c,t} = \frac{\dot{u}_r}{r} = \frac{|z - z_{ICR}| \cdot \dot{\psi}}{r} \qquad \text{with } z_{ICR} < z \leq d \tag{10}$$

Substituting (9) and (10) in (8), the rate of internal energy dissipated in concrete tangential compression may be computed as:

$$P_{i,c,t} = -\int_{z_{ICR}}^{d} \int_{0}^{2\cdot\pi} \int_{r_c}^{r_s} \frac{|z - z_{ICR}|}{r} \cdot f_{cp} \cdot \dot{\psi} \cdot r \cdot dr \cdot d\vartheta \cdot dz = -\pi \cdot (r_s - r_c) \cdot \langle d - z_{ICR} \rangle^2 \cdot f_{cp} \cdot \dot{\psi} \tag{11}$$

where $\langle d - z_{ICR} \rangle$ is equal to zero when the component $d - z_{ICR}$ is negative. This component does not exist in mechanism M2, since the entire footing is considered to be in tension in the corresponding kinematics.

3.4 Rate of internal of energy dissipated in the reinforcement

A velocity with a non-zero radial component at the level of both bottom and top reinforcement may occur in both mechanisms. In those cases, dissipation of energy occurs in the reinforcement, either in tension or in compression. The rate of internal energy dissipated in the bottom reinforcement results from the sum of rate of internal energy dissipated in both radial and tangential directions. With respect to radial direction, the rate of internal energy dissipated is given by:

$$P_{i,s,b}^{rad} = -\int \dot{u}_{r,s,b} \cdot f_y \cdot dA \tag{12}$$

where the radial component of the velcoity at the level of bottom reinforcement and the unit of area are respectively given by:

$$\dot{u}_{r,s,b} = \dot{u}_{r(z=0)} = \left|z_{ICR}\right| \cdot \dot{\psi} \tag{13}$$

$$dA = \rho \cdot r_0 \cdot d\vartheta \tag{14}$$

In what respects tangential direction, the rate of internal energy dissipated is given by:

$$P_{i,s,b}^{\tan} = -\int \dot{\varepsilon}_{t,s,b} \cdot f_{cp} \cdot dVol \tag{15}$$

where the corresponding strain rate and unit of volume given respectively by:

$$\dot{\varepsilon}_{t,s,b} = \frac{\dot{u}_{r,s,b}}{r} = \frac{\left|z_{ICR}\right| \cdot \dot{\psi}}{r} \tag{16}$$

$$dVol = \rho \cdot d \cdot r \cdot dr \cdot d\vartheta \tag{17}$$

Using (12) to (17), the rate of internal energy dissipated in the bottom reinforcement may be written as:

$$P_{i,s,b} = P_{i,s,b}^{rad} + P_{i,s,b}^{\tan} = -\int_0^{2\cdot\pi} \left|z_{ICR}\right| \cdot f_y \cdot \rho \cdot d \cdot r_0 \cdot \dot{\psi} \cdot d\vartheta - \int_0^{2\cdot\pi}\int_{r_0}^{r_s} \left|z_{ICR}\right| \cdot f_y \cdot \rho \cdot d \cdot \dot{\psi} \cdot dr \cdot d\vartheta \tag{18}$$

which may be simplified to:

$$P_{i,s,b} = -2\pi \cdot d \cdot f_{cp} \cdot r_s \cdot \omega \cdot \left|z_{ICR}\right| \cdot \dot{\psi} \tag{19}$$

where ω represents the bottom mechanical reinforcement ratio ($\omega=\rho\, f_y/f_{cp}$). The rate of internal energy dissipated in the top reinforcement may be analogously calculated:

$$P_{i,s,b} = -2\pi \cdot d \cdot f_{cp} \cdot \omega' \cdot r_s \cdot \left|z_{ICR} - \left(d - d'\right)\right| \cdot \dot{\psi} \tag{20}$$

where ω' refers to the top mechanical reinforcement ratio, computed as $\omega'=\rho'\, f_y/f_{cp}$.

3.5 Determination of load carrying capacity

The load carrying capacity may be calculated based on the kinematical theorem of limit analysis, provided that a location for the instantaneous centre of rotation and a geometry for the failure surface are assumed. The solution is the result of the minimization of the load carrying capacity. Besides the possibility of solving this problem by calculus of variations, using Lagrange-Euler equations (Courant & Hilbert 1953) as shown by Braestrup & al. (1976), it may be also numerically solved, corresponding to a constrained non-linear optimization problem (location of instantaneous centre of rotation and velocity field constrained). The results presented in the following were obtained through numerical optimization.

3 Discussion of theoretical results

The normalized load carrying capacity is shown in Fig. 6(a) as a function of the bottom mechanical reinforcement ratio and considering both potential mechanisms, for a general case characterized by r_s/d=2.0, r_q/d=1.5, r_c/d=0.3, $r_{0,max}$=1.3 and without top reinforcement (ω'=0). Several failure mechanisms are represented in Fig. 6(b) to (d), where the principal strain rate directions and the length of the regimes along the failure surface are also shown. The flexural capacity is also presented in Fig. 8(a), which was calculated according to:

$$V_{flex} = 2 \cdot \pi \cdot m_R \cdot \frac{r_s}{r_q - r_c} \tag{21}$$

where the flexural strength of the section m_R is computed assuming a rigid-plastic behaviour for concrete and steel:

$$m_R = f_{cp} \cdot \omega \cdot d^2 \cdot \left(1 - \frac{c}{2 \cdot d}\right) \tag{22}$$

where c represents the height of the compression zone which, in the cases where no top reinforcement is used, is equal to $c=\omega d$. It is shown in Fig. 6(a) that a pure flexural failure occurs only in the cases where fairly low amounts of bottom mechanical reinforcement ratio are available. In these cases, the load carrying capacity obtained with mechanism M1 is very close to the one calculated according to (21) and (22). With increasing amount of bottom mechanical reinforcement ratio, two different regimes may be observed: (i) flexural-shear regime and (ii) punching shear regime. The first regime is characterized by an increase of the load carrying capacity with increasing amount of the bottom mechanical reinforcement ratio. Mechanism M1, which presents a kinematics with a counter-clockwise rotation (known to occur in pure flexural failures), is governing for a significant part of the flexural-shear regime. This regime defines a transition between a pure flexural failure and a punching shear failure. The rotation component of the failure mechanism reduces with increasing amount of bottom mechanical reinforcement ratio, decreasing the relative significance of rate of internal energy dissipated in the bottom reinforcement. On the other hand, the amount of energy dissipated along the failure surface increases as the length of regimes A and B along the failure surface also increases (refer to Fig. 6(b) and (c)). Therefore, while for low amounts of the bottom mechanical reinforcement ratio the location of the instantaneous centre of rotation is close to the footing (leading to an important component of rotation at failure), it is located at larger distances for increasing amounts of this reinforcement. This leads to a failure mechanism with low significance of rotation and a more significant component of translation.

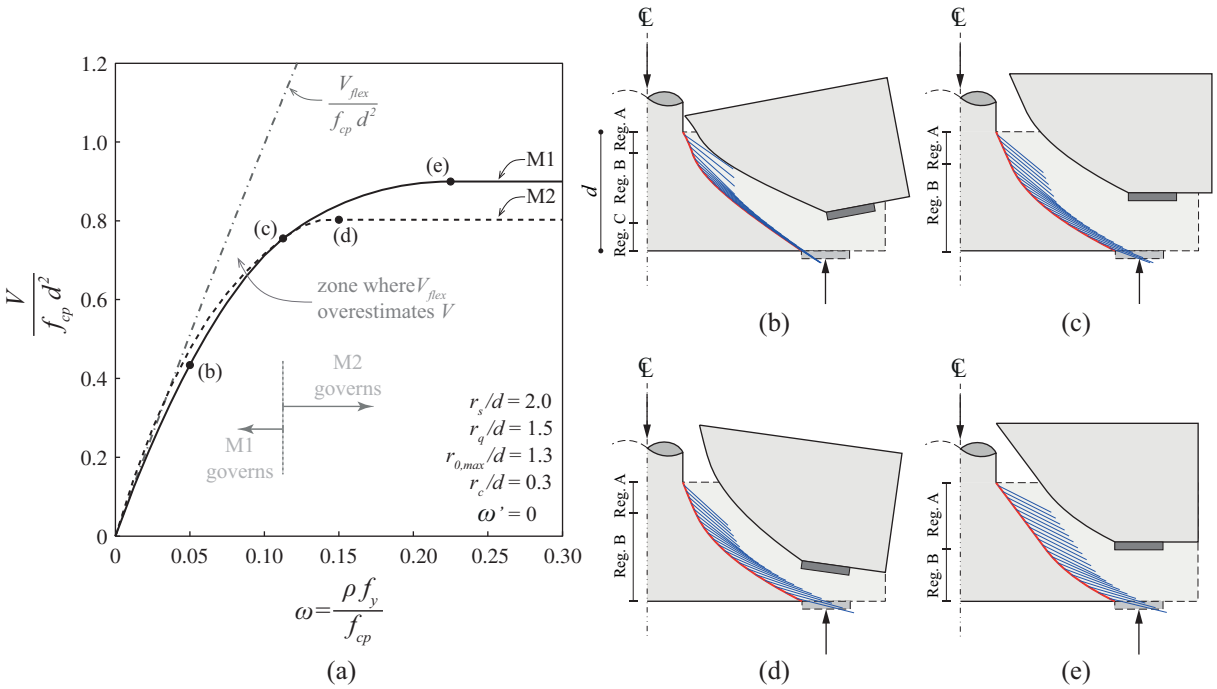

Fig. 6 (a) Normalized load carrying capacity as a function of the bottom mechanical reinforcement ratio for a general case with $r_{s/d}$=2.0, $r_{q/d}$=1.5, $r_{0,max}$=1.3, r_c/d=0.3 and ω'=0; (b) failure mechanism M1 for ω=0.05; (c) failure mechanism M1 and M2 for ω≈0.1125; (d) failure mechanism M2 for ω=0.15 and (e) failure mechanism M1 for ω=0.225.

The transition between mechanism M1 and M2 occurs when the failure mechanism is characterized by only a translational movement, meaning that in both cases the instantaneous centre of rotation is located at infinite (Fig. 6(c)). Thereafter, the increase of the bottom mechanical reinforcement ratio leads to a reduction in the radial component of the velocity in mechanism M1, thus decreasing the relative significance of the activation of the bottom reinforcement in the total rate of internal energy dissipated (at same time, the rate of internal energy dissipated in the concrete along the failure surface increases, compare Fig. 6(c) and (e)). In mechanism M2, the increase of the bottom mechanical reinforcement ratio leads to a progressive approximation of the instantaneous centre of rotation to the level of the bottom reinforcement and to the footing (leading to a clockwise rotation, compare Fig. 6(c) and (d)). While M1 leads to a failure mechanism characterized by a vertical translation of the outer portion of the footing when large amounts of bottom mechanical reinforcement ratio are provided, mechanism M2 leads to a failure mechanism with a clockwise rotation (instantaneous centre of rotation at the level of the bottom reinforcement). The load carrying capacity obtained in both cases is only governed by the energy dissipated along the failure surface. Nevertheless, from the comparison of Fig. 6 (d) and (e), it might be seen that mechanism M1 leads to a more significant presence of regime A (biaxial compression) along the failure surface. This result shows that the mechanism originally proposed by Braestrup & al. (1976), and later used by other researchers (Jiang & Shen 1986; Bortolotti 1990; Kuang 1991; Salim & Sebastian 2002), might not be the only one governing in punching shear failures. This is for instance the cases of compact footings without top reinforcement, since in these cases the instantaneous centre of rotation may get closer to the failure surface and no top reinforcement is available to be activated with a clockwise rotation. In these cases, if top reinforcement is provided, a change in the failure mechanism (reduction the clockwise rotational component) and an increase of the load carrying capacity may be observed. Therefore, a certain amount of top reinforcement (which is a function of geometrical and material properties) has apparently to be provided to ensure that a failure mechanism characterized by a vertical movement of the outer portion of the footing is governing in the punching shear regime. This result may also be physically explained with the confinement stresses that top reinforcement may provide to the diagonal compression strut carrying shear (Guiddoti, Fernández Ruiz & Muttoni, 2010).

It is still important to note that, as already observed by Braestrup & al. (1976), the failure surface develops in between the column edge and the support inner radius, since the tensile strength of concrete is neglected. Therefore, the support width assumes an important role not only for the mechanism M1, but mostly for the mechanism M2, specifically in the cases where top compression reinforcement is not provided.

It can also be noted that the approach presented above can be extended to other cases, varying the geometrical and material properties as well as the reactions distribution (e.g. uniform soil reaction).

4 Comparison between theoretical and experimental results

Hallgren, Kinnunen and Nylander (1998) is one of the several experimental works performed presented having as objective the investigation of the punching shear behaviour of footings (e.g. Talbot 1913; Richart 1948; Kordina & Nölting 1981; Dieterle 1986; Dieterle & Rostásy 1987; Hallgren & Bjerke 2002; Timm 2003; Hegger, Sherif & Ricker 2006; Hegger & al. 2007; Hegger, Ricker & Sherif 2009; Ricker 2006; Siburg & Hegger 2014; Urban & al. 2013). Hallgren, Kinnunen & Nylander (1998) performed tests on eleven reinforced concrete column footings without shear reinforcement that showed the influence of the bottom reinforcement ratio and of the concrete compressive strength. It was concluded that the concrete compressive strength has an important influence in the footings load capacity, significantly higher than in slender slabs, and that the influence of the longitudinal reinforcement ratio was not so pronounced as for the concrete compressive strength. Three additional investigated parameters were the type of anchorage of the reinforcement bars, the type of loading (line or uniform) and the shape of the footing (square or circular). According

to Hallgren, Kinnunen & Nylander (1998), these three parameters do not have a significant influence in the value of the collapse load.

The work presented by Hallgren, Kinnunen and Nylander (1998) is used here to compare the experimental results with the theoretical predictions using the kinematical approach above presented. This experimental campaign presents nine tests (S1 to S5, S7 to S9, S12 and S13) with the same loading setup (concentrated reactions) and where all the parameters (r_s, r_c, r_q, d, ω') were kept approximately constant, varying only the bottom mechanical reinforcement ratio ω. In the present analysis it is considered that the loading plates had a diameter equal to 0.10 m. The main properties for each test are presented in Table 1.

The theoretical prediction calculated using the kinematical approach above presented as well as the ratio $V_{R,test} / V_{R,Plastic}$ obtained for each experimental result are presented in Table 1. The value of the plastic concrete compressive strength f_{cp} was calculated according to (1) assuming η_{fc} from (2) and η_ε=0.55. This latter value is selected according to the reduction factor proposed by *fib* Model Code 2010 to take into account the shear cracking developing not parallel to the compression direction (typical case of beams with shear reinforcement where limit analysis is used by means of the truss analogy). The results of the ratio $V_{R,test} / V_{R,Plastic}$ shows a fairly good agreement, with an average of 0.98 and a coefficient of variation of 0.085.

Table 1
Description of experimental tests performed by Hallgren, Kinnunen and Nylander (1998)

Specimen	Shape	r_s [1] [mm]	r_c [2] [mm]	r_q [3] [mm]	d [mm]	$f_{c,cube}$ [4] [MPa]	ρ [%]	f_y [Mpa]	$V_{R,test}$ [MN]	f_{cp} [MPa]	ω	$V_{Plastic}$ [MN]	$V_{R,test} / V_{R,Plastic}$
S1	square	480	125	337	242	49.8	0.40	621	1.36	19.9	0.13	1.34	1.02
S2					243	35.5	0.40		1.02	15.6	0.16	1.10	0.92
S3					250	37.2	0.39		1.01	16.4	0.15	1.20	0.84
S4					232	32.1	0.66		0.99	14.1	0.29	0.94	1.06
S7					246	18	0.40		0.62	7.9	0.31	0.57	1.09
S8					245	39.3	0.25		0.92	17	0.09	0.98	0.93
S9					244	31.9	0.40		0.90	14	0.18	1.00	0.91
S12	circular	480		337	242	34.1	0.42		1.05	15	0.17	1.05	0.99
S13					244	24.7	0.42		0.80	10.9	0.24	0.77	1.04
												Average	0.98
												COV	0.085

{1} for square footings, r_s is calculated considering an equal area for the bottom surface;
{2} circular columns used in all the specimens;
{3} for square footings, r_q is simplified considering to be equal to the one of the experimental tests in circular footings;
{4} to compare with the theoretical results, an f_c =0.8 $f_{c,cube}$ is considered.

Fig. 7(a) depicts the normalized load carrying capacity as a function of the bottom mechanical reinforcement ratio considering an average value for the effective depth of d=0.243 m (therefore leading to definition of the parameters characterizing this experimental campaign with the following average values: r_c/d=0.514; r_s/d=1.98; r_q/d=1.39; $r_{0,max}/d$=1.18 and ω'=0). Also the flexural capacity, computed according to (21), is represented in Fig. 7(a). Although the theoretical curves shown in Fig. 7(a) represent average values, a good agreement between theoretical and experimental results may be observed, in accordance with the results already presented in Table 1. Nevertheless, it might be seen that the plastic solution tends to slightly overestimate the experimental load capacity for low amounts of the bottom mechanical reinforcement ratio and to underestimate for larger amounts of this ratio. The ratio $V_{R,test} / V_{R,Plastic}$ obtained for each experimental test (refer to Table 1) is shown in Fig. 7(b) as a function of the bottom mechanical reinforcement ratio, being possible to observe a slight increase of this ratio with increasing the bottom mechanical reinforcement ratio. This result may be physically explained by the fact that footings with low amounts of bottom mechanical reinforcement ratio present

a softer behaviour (larger deformations), therefore requiring a more pronounced reduction of the concrete compressive strength. On the other hand, footings with large amounts of bottom reinforcement ratio present a stiffer behaviour, requiring slightly lower reductions of the concrete compressive strength.

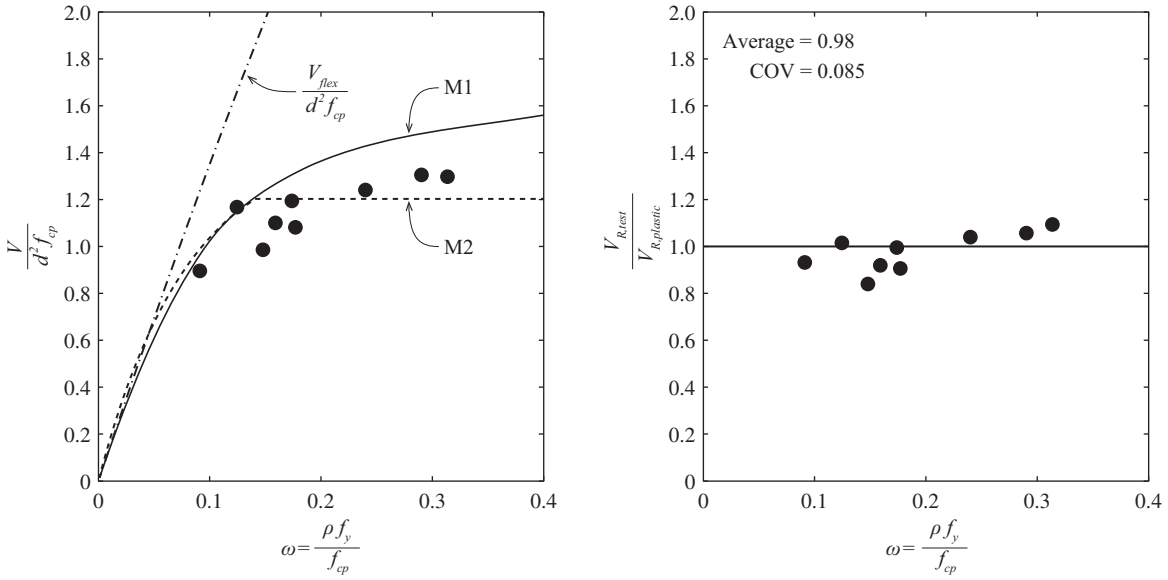

Fig. 7 (a) Comparison between proposed plastic solution and experimental values of load carrying capacity as a function of bottom mechanical reinforcement ratio for the experimental tests of Hallgren, Kinnunen and Nylander (1998), considering the following average values: r_c/d=0.514; r_s/d=1.98; r_q/d=1.39; $r_{0,max}/d$=1.18 and ω'=0 with d = 0.243m; (b) ratio $V_{R,test}/V_{R,plastic}$ as a function of bottom mechanical reinforcement ratio.

5 Conclusions

A kinematical approach is proposed to calculate the load carrying capacity of isolated footings under concentrated reactions. Rigid-plastic behaviour, based on a Mohr-Coulomb yield criterion, was adopted for the concrete, being its tensile strength neglected. The reinforcement bars are considered to behave in a rigid perfectly plastic manner in both tension and compression. Two different mechanisms, referring to different kinematics, are considered. The following conclusions are obtained:

1) Besides the flexural regime observed for very low amounts of bottom mechanical reinforcement, two regimes may govern: (i) flexural-shear and (ii) punching shear regime;

2) The flexural-shear regime, which is shown to lead to lower strength than the one obtained considering a pure flexural failure, governs for low amounts of the bottom mechanical reinforcement and represents a smooth transition between pure flexural and punching shear failures;

3) The punching shear failure is governing for large amounts of bottom mechanical reinforcement;

4) It is shown that top compression reinforcement might play an important role in the punching shear regime; the punching shear failure is characterized by a vertical movement of the outer portion of the footing when large amounts of top reinforcement is used; when top reinforcement is not provided, a failure mechanism with an instantaneous centre of rotation close to the footing and at the level of the bottom flexural reinforcement might govern;

5) The approach presented in this paper is shown to be consistent with the experimental results of Hallgren, Kinnunen and Nylander (1998), considering a reduction factor of η_ε=0.55 to take into account the presence of transverse strains; this corresponds to a value normally used when limit analysis is applied to shear strength problems.

References

Braestrup, M. W. (1974), Plastic analysis of shear in reinforced concrete. Magazine of Concrete Research, Vol. 26, No. 89, pp. 221-228.

Braestrup, M. W. (1979), Punching shear in concrete slabs. Plasticity in Reinforced Concrete, Session III, Colloquium of International Association for Bridge and Structural Engineering, Copenhagen, Vol. 28, pp. 115–136.

Braestrup, M. W. (1981), Structural concrete as a plastic material. In IABSE Colloquium Advanced Mechanics of Reinforced Concrete, Delft, pp. 3-16.

Braestrup, M. W., Nielsen M. P., Jensen B. C. & Bach F. (1976), Axisymetric Punching of Plain and Reinforced Concrete. Report No. 75, Structural Research Laboratory, Technical University of Denmark.

Bortolotti, L. (1990), Punching Shear Strength in Concrete Slabs. ACI Structural Journal, Vol. 87, No. 2, pp. 208-219.

Chen, W.-F. (2007), Plasticity in reinforced concrete. J. Ross Publishing.

Collins, M. P., Mitchell, D., Adebar, P. & Vecchio, F. J. (1996), A General Shear Design Method. ACI Structural Journal, Vol. 93, No. 1, pp. 36-45.

Courant, R. & Hilbert, D. (1953), Method of Mathematical Physics. John Wiley & Sons, Interscience Publishers, Vol. 1.

Dieterle, H. (1987), Design of reinforced concrete foundations of square columns under centric loading with the help of design diagrams, Deutscher Ausschuss für Stahlbeton, Vol. 387, pp. 94-134 (In German: Zur Bemessung quadratischer Stützenfundamente aus Stahlbeton unter zentrischer Belastung mit Hilfe von Bemessungsdigrammen).

Dieterle, H. & Rostásy, F. (1987), Load-carrying behavior of isolated reinforced concrete foundations of square columns, Deutscher Ausschuss für Stahlbeton, Vol. 387, pp. 1-91 (In German: Tragverhalten quadratischer Einzelfundamente aus Stahlbeton).

Drucker, D. C. (1961), On Structural Concrete and the Theorems of Limit Analysis. IABSE International Association for Bridge and Structural Engineering, IABSE-Reports 21, Zürich, Switzerland.

Fernández Ruiz, M. & Muttoni, A. (2007), On Development of Suitable Stress Fields for Structural Concrete. ACI, Structural Journal, Vol. 104, No. 4, pp. 495-502.

Fernández Ruiz, M. & Muttoni, A. (2008), Shear strength of thin-webbed post-tensioned beams, ACI Structural Journal, Vol. 105, No. 3, pp. 308-317.

fib (2012), Model Code 2010 – final draft, vols. 1 and 2, *fib* Bulletin 65, 350p., *fib* Bulletin 66, 370p.

Gesund, H. (1983), Flexural Limit Analysis of Concentrically Loaded Column Footings. ACI Journal Proceedings, Vol. 80, No. 3, pp. 223-228.

Gesund, H. (1985), Flexural Limit Design of Column Footings. Journal of Structural Engineering, Vol. 111, No. 11, pp. 2273-2287.

Gesund, H. & Dikshit, O. P. (1971), Yield Line Analysis of the Punching Problem at Slab/Column Intersections. ACI Special Publication, Vol. 30, pp. 177-201.

Guidotti, R., Fernández Ruiz, M. & Muttoni, A. (2011), Crushing and Flexural Strength of Slab-Column Joints. Engineering Structures, Vol. 33, No. 3, pp. 855-867.

Hallgren, M., Kinnunen, S. & Nylander, B. (1998), Punching Shear Tests On Column Footings. Nordic concrete research, No. 21, pp. 1-22.

Hallgren M. & Bjerke M. (2002), Non-linear finite element analyses of punching shear failure of column footings. Cement and Concrete Composites, Vol. 24, No. 6, pp. 491-496.

Hegger, J., Ricker, M., Ulke, B. & Ziegler, M. (2007), Investigations on the punching behavior of reinforced concrete footings. Engineering Structures, Vol. 29, No. 9, pp. 2233-2241.

Hegger, J., Ricker, M. & Sherif, A. (2009), Punching Strength of Reinforced Concrete Footings. ACI Structural Journal, Vol. 106, No. 5, pp. 706-716.

Hegger, J., Sherif, A. & Ricker, M. (2006), Experimental Investigations on Punching Behavior of Reinforced Concrete Footings. ACI Structural Journal, Vol. 103, No. 4, pp. 604-613.

Jensen, B. C. (1975), Lines of discontinuity for displacements in the theory of plasticity of plain and reinforced concrete. Magazine of Concrete Research, Vol. 27, No. 2, pp. 143 –150.

Jiang, D.-H. & Shen, J.-H. (1986), Strength of Concrete Slabs in Punching Shear. Journal of Structural

Engineering, Vol. 112, No. 12, pp. 2578-2591.
Johansen, K.W. (1962), Yield-line Theory. Cement and Concrete Association, pp. 181.
Kuang, J. S. (1991), An Upper-bound Plastic Solution for Punching Shear Failure of Concrete Slabs. Report No. CUED/D-Struct/TR.136, Engineering Department, University of Cambridge, United Kingdom.
Kordina, K. & Nölting, D. (1981), Load-carrying behavior of eccentrically loaded isolated reinforced concrete foundations, Technical Report, DFG-Research Ko 204/27-30, Brunswick, Germany, pp. 158 (In German: Tragverhalten von ausmittig beanspruchten Einzelfundamenten aus Stahlbeton).
Muttoni, A. (1990), The applicability of the theory of plasticity to reinforced concrete design, Institut für Baustatik und Konstruction, Report No. 176, ETH Zurich, 159 pp. (In German: Die Andwendbarkeit der Plastizitätstheorie in der Bemessung von Stahlbeton).
Muttoni, A., Schwartz, J. & Thürlimann, B. (1997), Design of Concrete Structures with Stress Fields. Birkhäuser Verlag, Basel, Switzerland
Nielsen, M. P., Braestrup, M. W. & Bach, F. (1978), Rational analysis of shear in reinforced concrete beams. Plasticity in Reinforced Concrete, International Association for Bridge and Structural Engineering Periodica, IABSE Proceedings, Vol. 2, pp. 15-78, May.
Nielsen, M. P., Braestrup, M. W., Jensen, B. C. & Bach, F. (1978), Concrete Plasticity. Beam Shear – Shear in Joints – Punching Shear. Special Publication, Danish Society for Structural Science and Engineering.
Nielsen, M. P. & Hoang L. C. (2011), Limit Analysis and Concrete Plasticity. CRC Press, Boca Raton, Third Edition.
Richart, F. E. (1948), Reinforced Concrete Walls and Column Footings, Part 1 and 2. ACI Journal, Vol. 45, No. 2, pp. 97-127, pp. 237-260.
Ricker, M. (2006), Punching in RC Footings considering The Soil-Structure-Interaction. Proceedings of the 6th Int. Ph.D. Symposium in Civil Engineering, Zürich, Switzerland.
Salim, W. & Sebastian, W. M. (2002), Plasticity Model for Predicting Punching Shear Strengths of Reinforced Concrete Slabs. ACI Structural Journal, Vol. 99, No. 6, pp. 827-835.
Siburg, C. & Hegger, J. (2014), Experimental Investigations on Punching Behaviour of Reinforced Concrete Footings with structural dimensions. Structural Concrete, Vol. 15, No. 3, pp. 331-339.
Talbot, A. N. (1913), Reinforced Concrete Wall Footings and Column Footings. Engineering Experiment Station, University of Illinois , Bulletin 67.
Timm, M. (2003), Punching of foundation slabs under axisymmetric loading, Doctoral Thesis, Institute for Building Materials, Concrete Structures and Fire Protection of the Technical University Braunschweig, pp. 159 (In German: Durchstanzen von Bodenplatten unter rotationssymmetrischer Belastung).
Urban, T., Gołdyn, M., Krakowski, J., & Krawczyk, Ł. (2013), Experimental investigation on punching behavior of thick reinforced concrete slabs. Archives of Civil Engineering, Vol. 59, No. 2, pp. 157-174.
Vecchio, F. J. (2000), Disturbed stress field model for reinforced concrete: formulation. Journal of Structural Engineering, Vol. 126, No. 9, pp. 1070-1077.
Vecchio, F. J. & Collins, M. P. (1986), The modified compression-field theory for reinforced concrete elements subjected to shear. ACI Journal, Vol. 83, No. 2, pp. 219-231.
Vecchio, F. J. & Collins, M. P. (1988), Predicting the Response of Reinforced Concrete Beams Subjected to Shear Using Modified Compression Field Theory. ACI Structural Journal, Vol. 85, No. 3, pp. 258-268.